Electronic Supplementary Information

2D Quasi-ordered Nitrogen-enriched Porous Carbon Nanohybrids for High Energy Density Supercapacitors

Kan Kan,[a, b] Lei Wang,[a*] Peng Yu,[a] Baojiang Jiang,[a] Keying Shi,[a] and Honggang Fu[*a]

[a] *Key Laboratory of Functional Inorganic Material Chemistry Ministry of Education of the People's Republic of China, Heilongjiang University, Harbin 150080 (P.R. China)*

[b] *Daqing Branch, Heilongjiang Academy of Sciences, Daqing 163319 (P.R. China)*

E-mail: fuhg@vip.sina.com; wanglei0525@126.com.

Fax: (+86) 451 8666 1259; Tel: (+86) 451 8660 4330.

1. Structural Characterizations

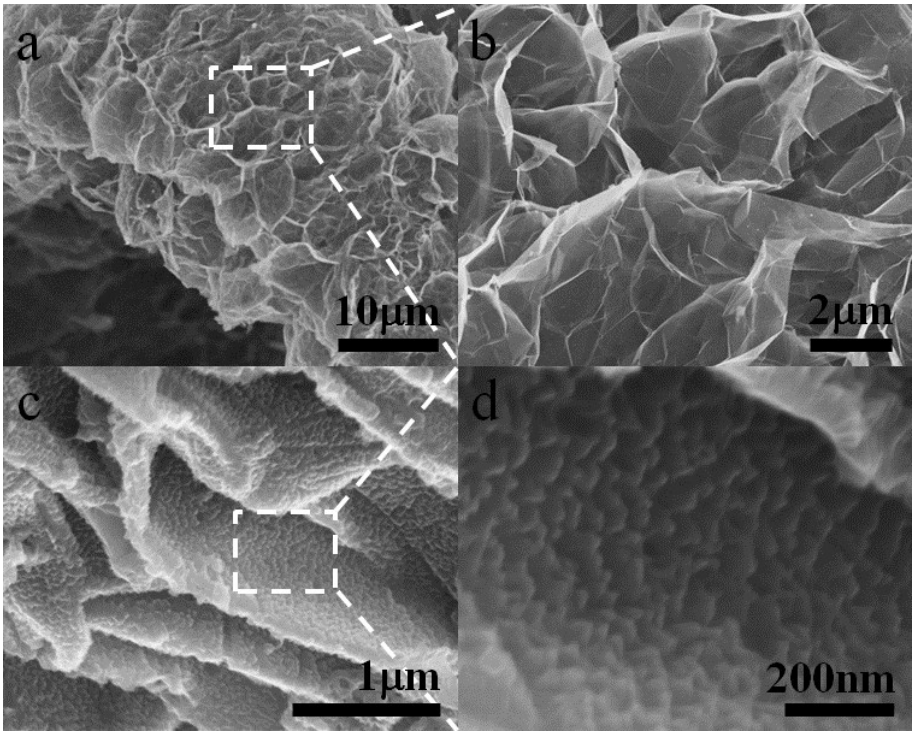

Fig. S1 (a, b) SEM images of EG. (c, d) SEM images of PANI/EG12.

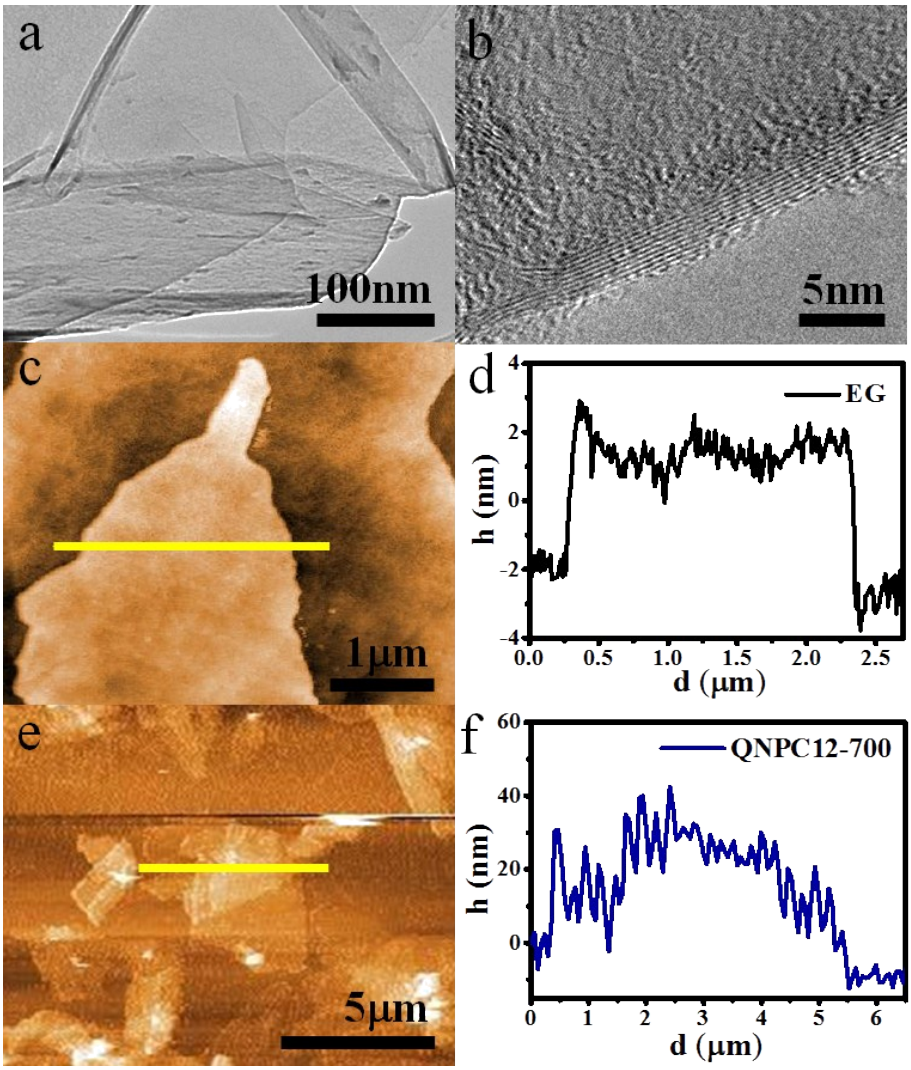

Fig. S2 (a, b) TEM images of expanded EG. AFM images of (c) expanded EG and (e) QNPC12-700, (d, f) are the corresponding thickness analysis of the yellow line in the (c, e), respectively.

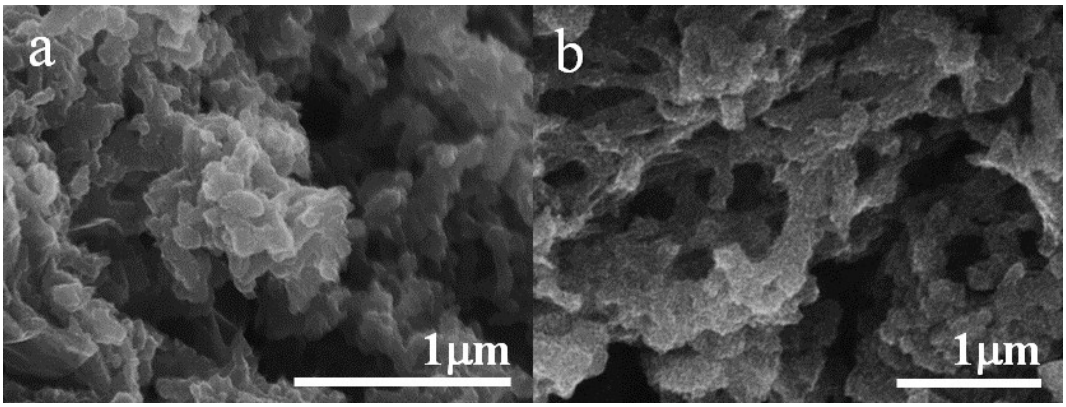

Fig. S3 SEM images of PANI (a) and NC-700 (b) samples.

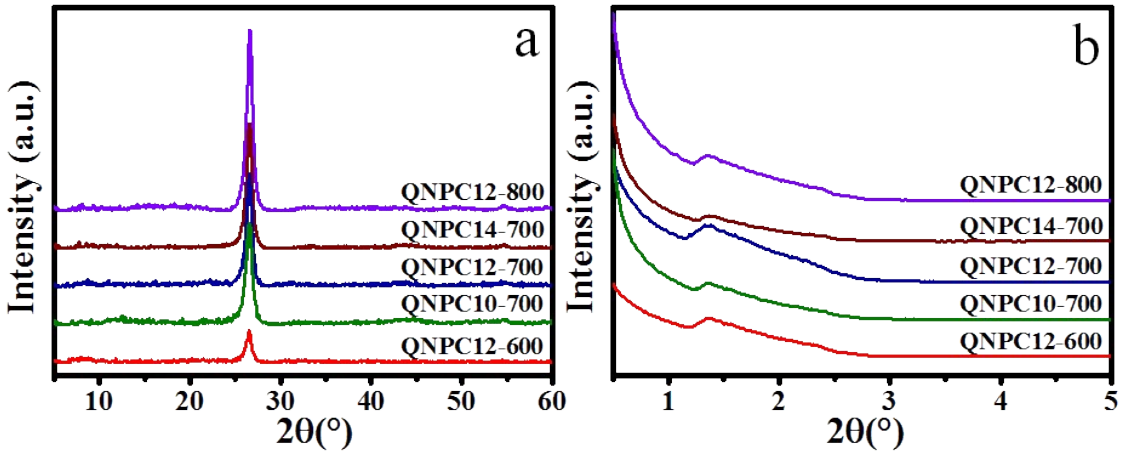

Fig. S4 (a) Wide-angle XRD and (b) small-angle XRD patterns of QNPC12-800, QNPC14-700, QNPC12-700, QNPC10-700 and QNPC12-600 nanohybrids.

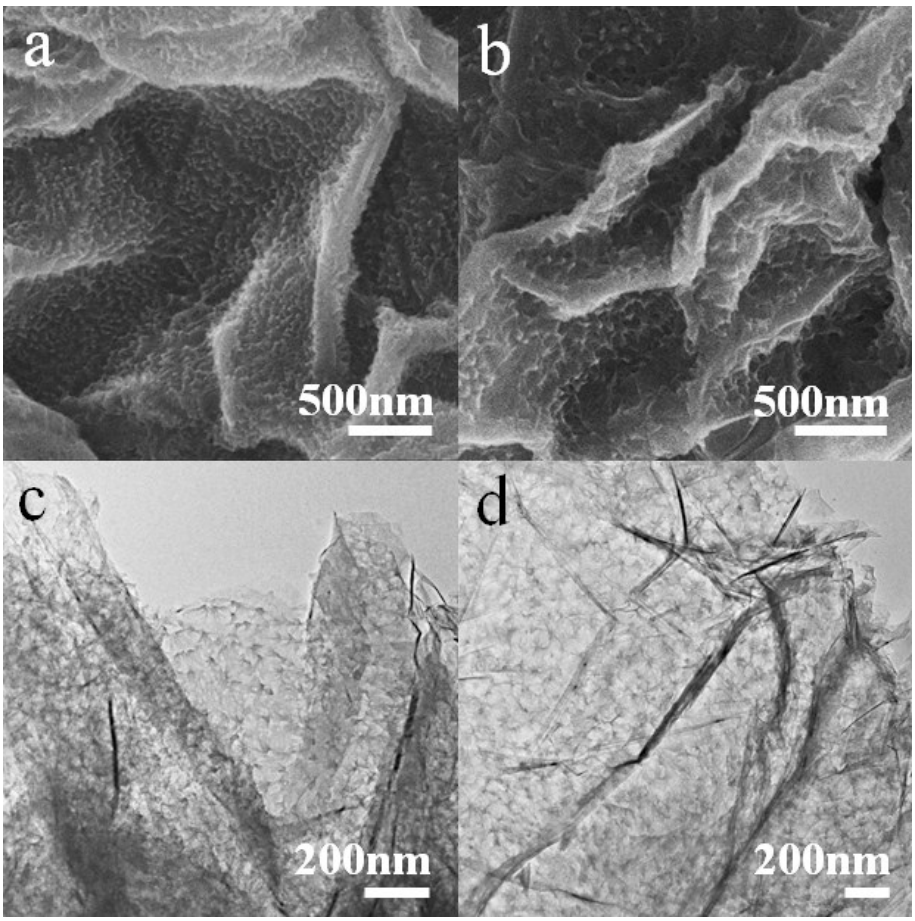

Fig. S5 The morphology of the QNPC nanohybrids derived from different carbonized temperatures: SEM images of (a) QNPC12-600 and (b) QNPC12-800; TEM images of (c) QNPC12-600 and (d) QNPC12-800.

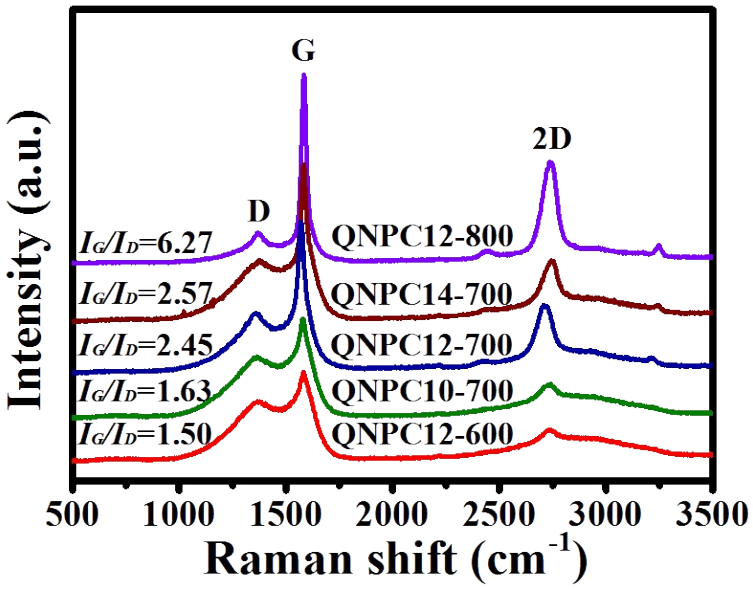

Fig. S6 The Raman spectra of QNPC12-800, QNPC14-700, QNPC12-700, QNPC10-700 and QNPC12-600 nanohybrids.

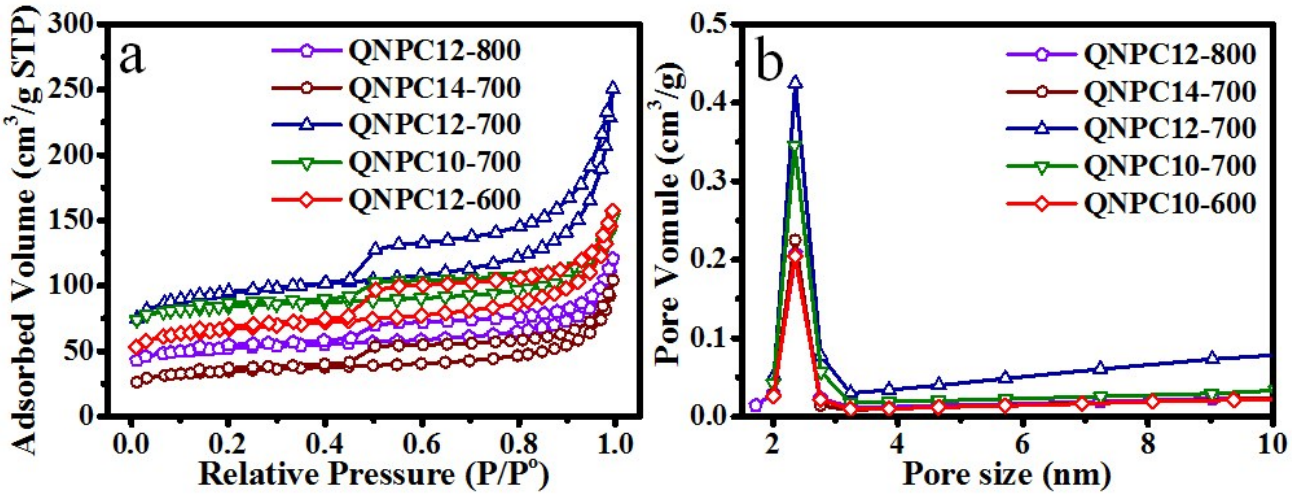

Fig. S7 (a) N_2 adsorption-desorption isotherms of QNPC12-800, QNPC14-700, QNPC12-700, QNPC10-700, and QNPC12-600 nanohybrids. (b) The corresponding DFT pore size distributions curves for the QNPC nanohybrids.

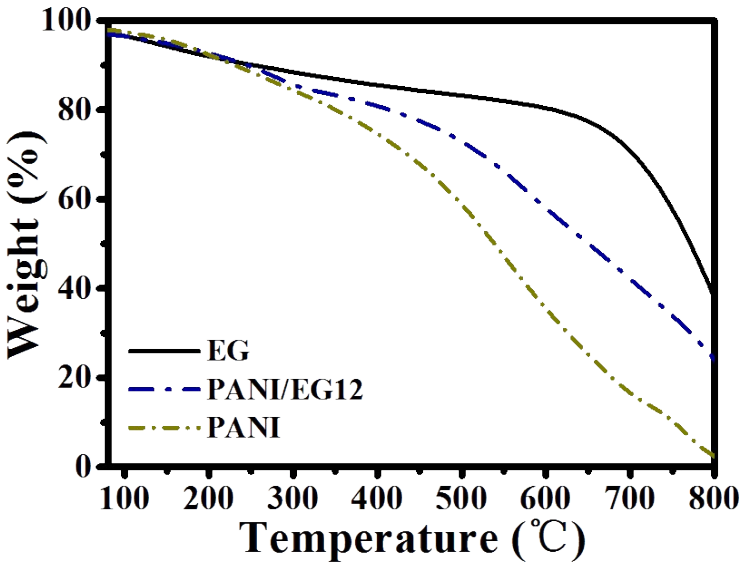

Fig. S8 TGA curves of EG, PANI/EG12 and PANI samples. The heating rate is 10 °C min^{-1} in N_2.

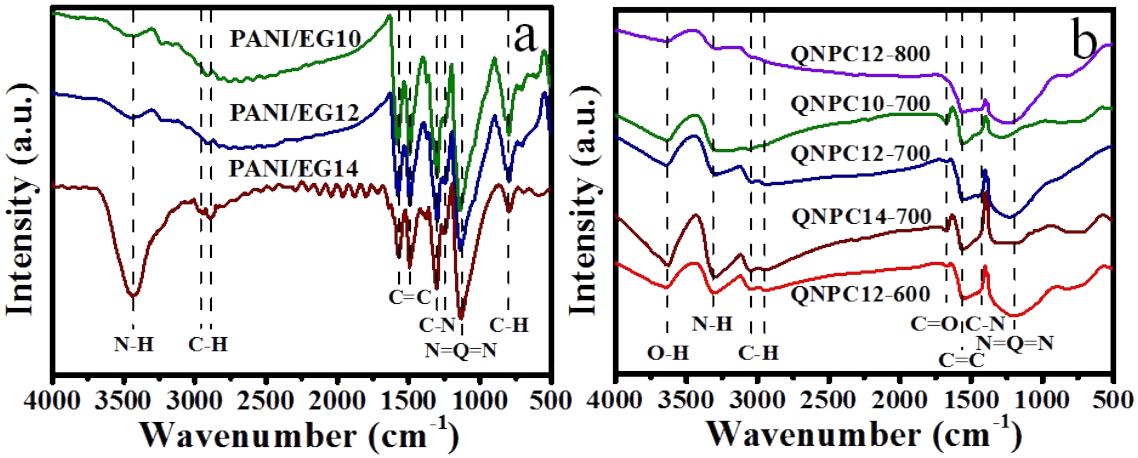

Fig. S9 (a) FTIR spectra of PANI/EG10, PANI/EG12, and PANI/EG14 nanohybrids. (b) FTIR spectra of QNPC12-800, QNPC10-700, QNPC12-700, QNPC14-700 and QNPC12-600 nanohybrids.

2. The Effect of Nitrogen-doping on Electrochemical Performance

In order to investigate the effect of nitrogen content on capacitance, three methods are selected to remove the doped nitrogen from QNPC12-700. The detailed experimental method, results and descriptions are as follows:

(1) Treated the QNPC12-700 sample by the digestion reaction: 0.2 g QNPC12-700 and 0.2 g Na_2SO_4 were added to 20 ml concentrated H_2SO_4. The mixed solution was heated to 150 °C and stirring for 1 h. Then, the obtained samples were washed with deionized water until the filtrate became neutral and dried at 80 °C for 24 h, which is denoted as QNPC12-700-a. Although the digestion reaction may make the doped nitrogen transfer into $(NH_4)_2SO_4$, the nitrogen content of QNPC12-700-a only decrease from 5.22 to 4.85 at.% as evidenced by XPS measurement (Fig. S10a and Table S1). In XPS spectrum, the distinct oxygen element can be observed, indicating that oxygen is introduced during the digestion reaction. It should be noted, however, that not only nitrogen but also carbon in QNPC12-700 participates in the reaction; thereby, compared with QNPC12-700, the structure of 2D planar nanosheets covered with quasi-ordered tower-like carbon layer damages seriously, which also leads to the reduction of S_{BET} (as shown in Fig. S11a, S12, and Table S1). The specific capacitance of QNPC12-700-a electrode indeed decreases significantly relative to QNPC12-700 (114.4 F g^{-1} for QNPC12-700-a, and 305.7 F g^{-1} for QNPC12-700) (Fig. S13 and Table S1). The drastic decline in specific capacitance mainly stems from the reduction of S_{BET}.

(2) Treated PANI/EG12 precursor by the diazo reaction: 0.1 g PANI/EG12 was added to 50 mL 4 mol L^{-1} HCl, and cooled to 0-5 °C with stirring for 30 min. 5 mL deionized water containing 0.73 g $NaNO_2$ was droped into the above solution slowly and stirred for 30 min. After washing with deionized water to the neutral, the treated PANI/EG12 was carbonized and chemical activated by the same procedure. The obtained sample is named as QNPC12-700-b. The diazo reaction is an effective strategy to transfer aniline to phenol. Therefore, we treated PANI/EG12 precursor by using HCl and $NaNO_2$ before pyrolysis and activation processes. There is almost no change in morphology, but the S_{BET} are decreased slightly from 348.4 to 298.6 m^2 g^{-1} (Fig. S11b, S12, and Table S1). The nitrogen content of QNPC12-700-b derived from XPS test slightly reduced to 4.93 at.%, maybe due to only the amino group at the ends of the polymer chain and oligomer molecule chain of PANI being removed during the diazo

reaction. As mentioned in the original manuscript, among various N-doping types in QNPC12-700, the N-6 and N-5 play the important role for providing the pseudo-capacitance effect, while the N-Q with positive charge can greatly affect the electron transfer. Compared with QNPC12-700, the peak area ratio of N-6 in QNPC12-700-b reduced, indicating that the reduced N contents are from N-6 (Fig. S10b). Therefore, the corresponding specific capacitance reduced to 284.7 F g^{-1}, which is a result of both the reduced N-6 and S_{BET} (Fig. S13).

(3) Treated the QNPC12-700 with high-temperature pyrolysis reaction: The QNPC12-700 was heated in 1200 °C for 2 h under N_2 ambient with a heating rate of 10 °C min^{-1}, denoted as QNPC12-700-c. The high-temperature pyrolysis can drastically remove doped N (*e. g. J. Mater. Chem. A*, 2014, 2, 8859; *Chem. Eur. J.*, 2014, 20, 564, *etc.*). As shown in Fig. S10c and Table S1, the QNPC12-700-c sample has the lowest nitrogen contents of 1.31 at.% after being heated treatment in 1200 °C under N_2 ambient. The residual nitrogen in QNPC12-700-c sample mainly exists in the form of thermostable N-Q. The QNPC12-700-c exhibits no obvious changes in morphology, but the S_{BET} of QNPC12-700-c is decreased to 275.4 m^2 g^{-1} due to the collapse and shrinkage of pores at the high temperature (Fig. S11c, S12 and Table S1). These results further confirm that the main doped-nitrogen derived from PANI is N-5, N-6 and N-Q in the tower-like carbon layer, and the structure would be drastic damaged when removing the doped-nitrogen. Compared with QNPC12-700 electrode, QNPC12-700c electrode exhibits a relative lower capacitance and doesn't present obvious redox current at around -0.8 V, indicating that the reduced nitrogen-doping content has an impact on the pseudo-capacitance (Fig. S13).

Table S1 Elemental composition, textual parameters and electrochemical properties of QNPC12-700-a, QNPC12-700-b, QNPC12-700-c, and QNPC12-700.

Sample	XPS (at.%)			Textual parameters		C_g at 1.0 A g^{-1} ($F g^{-1}$)
	C1s	O1s	N1s	S_{BET} ($m^2 g^{-1}$)	Average pore size (nm)	
QNPC12-700-a	83.37	11.78	4.85	111.6	7.23	114.4
QNPC12-700-b	91.08	3.99	4.93	298.6	3.49	284.7
QNPC12-700-c	93.64	5.05	1.31	275.4	5.83	230.4
QNPC12-700	92.01	2.77	5.22	348.4	3.77	305.7

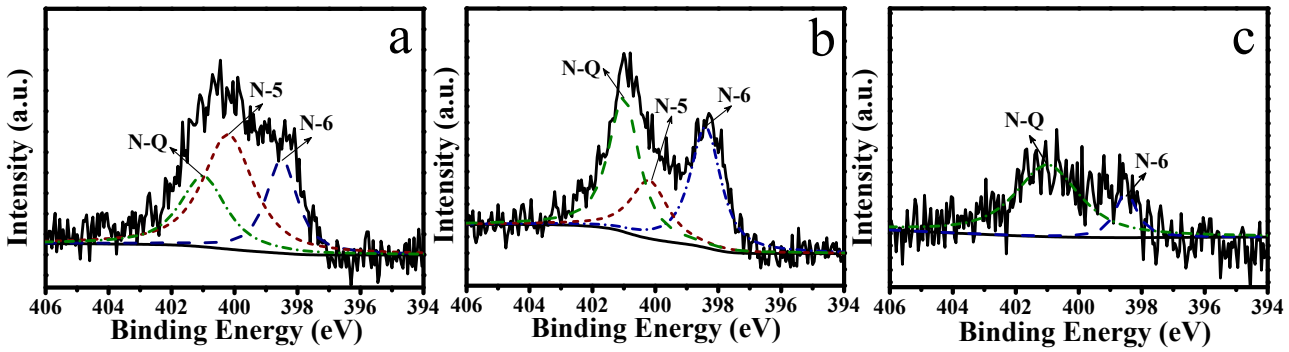

Fig. S10 XPS N1s spectra of (a) QNPC12-700-a, (b) QNPC12-700-b and (c) QNPC12-700-c.

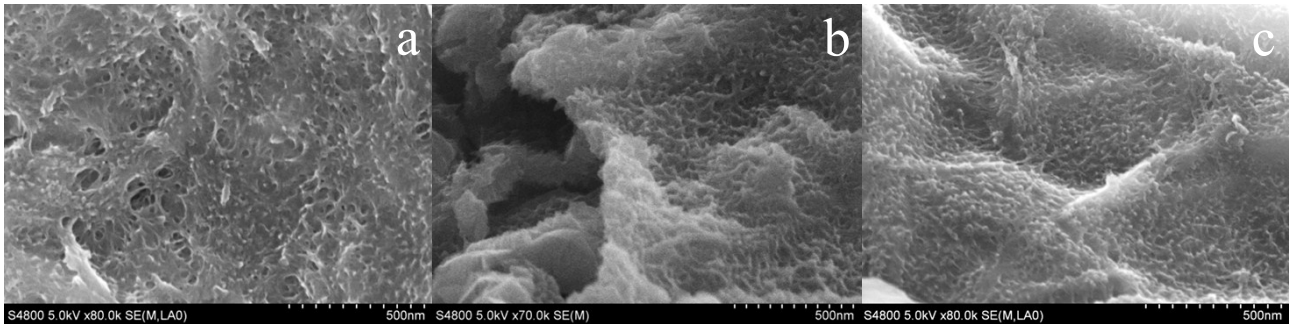

Fig. S11 SEM images of (a) QNPC12-700-a, (b) QNPC12-700-b and (c) QNPC12-700-c.

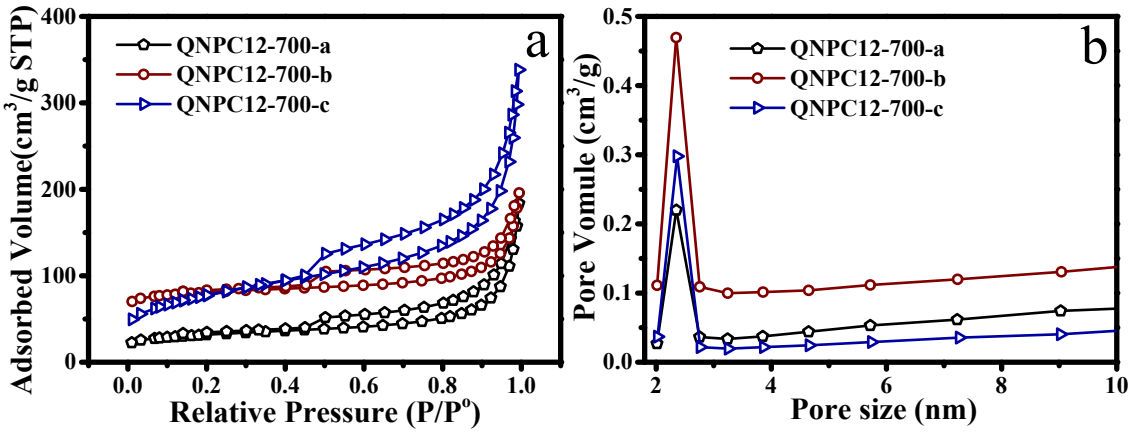

Fig. S12 (a) N_2 adsorption-desorption isotherms of QNPC12-700-a, QNPC12-700-b and QNPC12-700-c. (b) The corresponding DFT pore size distributions curves for the QNPC12-700-a, QNPC12-700-b and QNPC12-700-c.

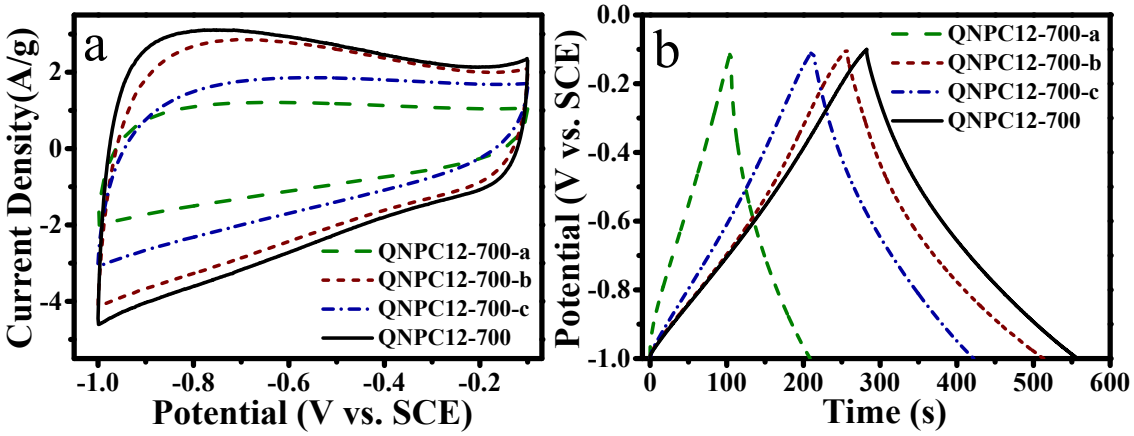

Fig. S13 Electrochemical properties of QNPC12-700-a, QNPC12-700-b, QNPC12-700-c and QNPC12-700 electrodes in 6 M KOH electrolyte: (a) CV curves at the scan rate of 10 mV s^{-1} in the potential range of -1.0 to -0.1 V (vs. SCE); (b) GCD tests of the materials at 1 A g^{-1}.

It is generally known that both the higher nitrogen-doping content and bigger S_{BET} are the main factors that produce larger specific capacitance. Therefore, just from three reference samples, it's hard to conclude that the difference in the specific capacitance mainly originates from the nitrogen-doping due to the synchronous decrease in S_{BET}. The main reason is that nitrogen has incorporated into the bulk of tower-like carbon layer during the carbonization, and the structure of tower-like carbon layer would be damaged when removing the doped-nitrogen. In order to further demonstrate the effect of nitrogen-doping for the improvement of capacitance, we have compared the present work with our previous work about mesoporous carbon coated graphite nanosheets (GNS@MC) without N-doping by the similar synthetic route derived from phenolic resin precursor and EG (Ref.[38]). The GNS@MC composite exhibits similar structural characteristics compared with QNPC12-700. Although the MCGNS composite has a higher S_{BET} of 432.3 m^2 g^{-1} than that of the QNPC12-700 (348.4 m^2 g^{-1}), its specific capacitance is much lower than that of QNPC12-700 (245.2 vs. 305.7 F g^{-1}), which further demonstrates that nitrogen-doping indeed plays critical role for the enhanced capacitance by providing pseudo-capacitance to a certain extent.

3. Electrochemical Performance

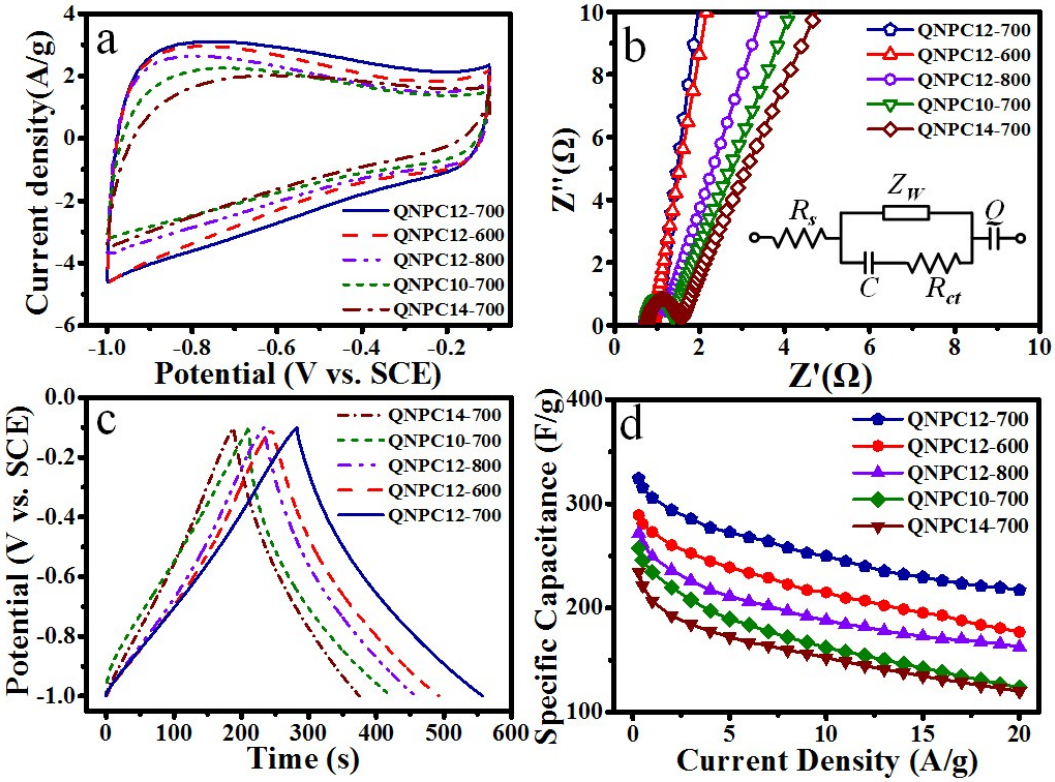

Fig. S14 Electrochemical properties of QNPC12-700, QNPC12-600, QNPC12-800, QNPC10-700 and QNPC14-700 electrodes in 6 M KOH electrolyte: (a) CV curves at the scan rate of 10 mV s^{-1} in the potential range of -1.0~0.2 V (vs. SCE); (b) Nyquist plots at a frequency from 10 mHz to 100 kHz; (c) GCD curves at the current density of 1 A g^{-1}; (d) the specific capacitances under various current densities from 0.3 to 20 A g^{-1}.

Table S2 The calculated values of R_s, R_{ct}, Z_W, C, and Q through CNLS fitting of the experimental impedance spectra based on the proposed equivalent circuit displayed in Fig. 7b and Fig. S10b.

Samples	R_s (Ω)	R_{ct} (Ω)	Z_W (Ω)	C (F)	Q (F)
QNPC12-700	0.2547	0.4122	0.1368	3.0453	1.8706
NC-700	1.3554	1.6934	1.1406	0.5562	0.2476
EG-700	0.4321	0.6176	1.0183	0.1201	0.1074

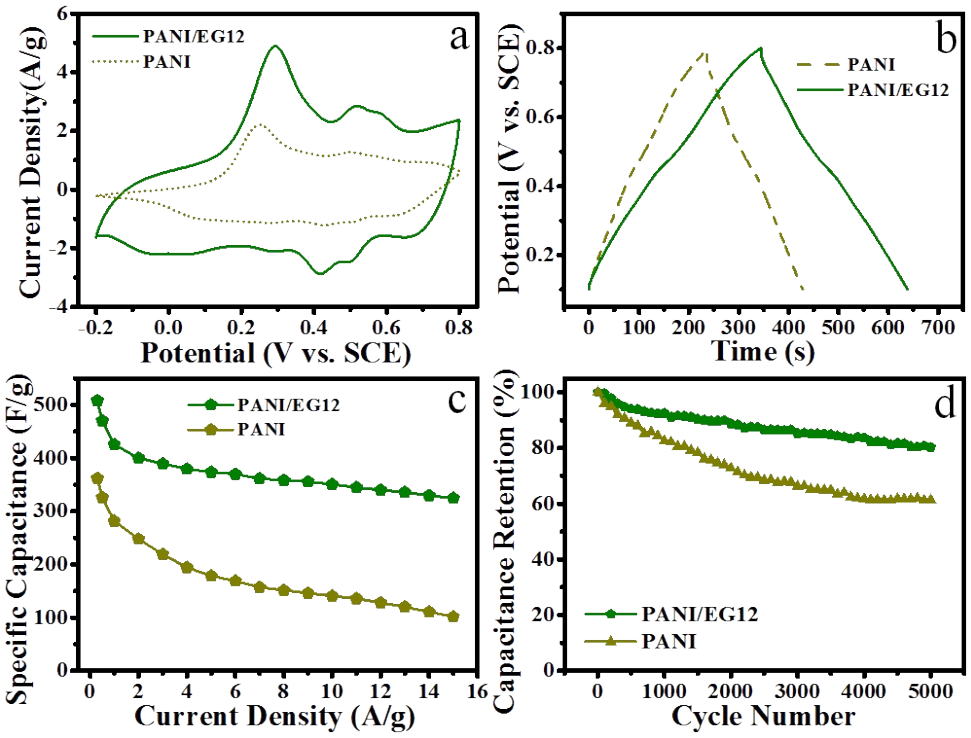

Fig. S15 Electrochemical properties of PANI and PANI/EG12 electrodes in 1 M H_2SO_4 electrolyte: (a) CV curves at the scan rate of 10 mV s^{-1} in the potential range of -0.2~0.8 V (vs. SCE). (b) GCD tests of the materials at 1 A g^{-1}. (c) The specific capacitance with various current densities from 0.3 to 15.0 A g^{-1}. (d) The cyclic stability for 5000 cycles in at a current density of 10 A g^{-1}.

Table S3. Specific capacitance of different graphene-like nanosheet based carbon materials.

Material	3-Electrode System		2-Electrode System		Energy Density (Wh kg^{-1})	Ref.
	Electrolyte	Capacitance (F g^{-1})	Electrolyte	Capacitance (F g^{-1})		
NPGC650	1 M H_2SO_4	405 (0.2 A g^{-1})	----	----	----	[30]
GNS@MC-35-800	6M KOH	203 (1.0 A g^{-1})	6M KOH	186.8 (1.0 A g^{-1})	11.5 (10 kW kg^{-1})	[38]
MCG1	6M KOH	242 (0.5 A g^{-1})	6M KOH	174.4 (1.0 A g^{-1})	15.5 (8.8 kW kg^{-1})	[50]
NPGC-2-900	6M KOH	293 (1.0 A g^{-1})	6M KOH	292 (1.0 A g^{-1})	8.1 (10.5 kW kg^{-1})	[51]
			1M Et_4NBF_4-PC	188 (1.0 A g^{-1})	47.5 (10.5 kW kg^{-1})	

Table S4. Specific capacitance of different carbon materials prepared by PANI pyrolysis.

Material	3-Electrode System		2-Electrode System		Energy Density (Wh kg^{-1})	Ref.
	Electrolyte	Capacitance (F g^{-1})	Electrolyte	Capacitance (F g^{-1})		
PNHCS	6M KOH	213 (0.5 A g^{-1})	----	----	----	[13]
a-NENCs	6M KOH	385 (1.0 A g^{-1})	6M KOH	358 (0.5 A g^{-1})	----	[14]
HPCT-4	----	----	6M KOH	365.9 (0.1 A g^{-1})	10.3 (45 W kg^{-1})	[42]
A-CNT	1M H_2SO_4	319 (1.0 A g^{-1})	1M H_2SO_4	145 (1.0 A g^{-1})	4.7 (1.3 kW kg^{-1})	[52]
			$EMIMBF_4$	140 (1.0 A g^{-1})	56.6 (4.4 kW kg^{-1})	